

# Peptide Oligomerization Memory Effects and Their Impact on the Physical Stability of the GLP-1 Agonist Liraglutide

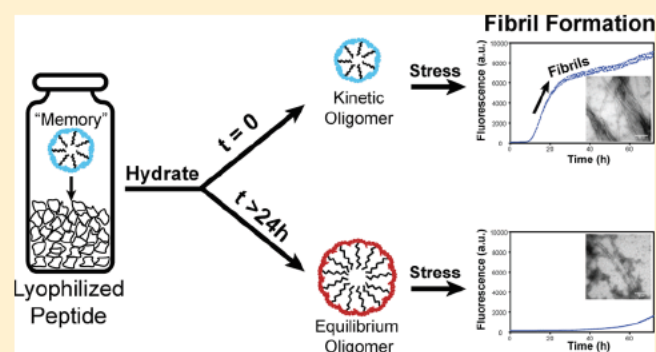
Jameson R. Bothe,<sup>\*,†</sup> Alexandra Andrews,<sup>§</sup> Katelyn J. Smith,<sup>§</sup> Leo A. Joyce,<sup>†</sup> Yogita Krishnamachari,<sup>§</sup> and Sandhya Kashi<sup>†</sup>

<sup>†</sup>Process Research and Development and <sup>§</sup>Pharmaceutical Sciences, Merck & Co., Inc., Rahway, New Jersey 07065, United States

## Supporting Information

**ABSTRACT:** Peptides and proteins commonly have complex structural landscapes allowing for transformation into a wide array of species including oligomers, aggregates, and fibrils. The formation of undesirable forms including aggregates and fibrils poses serious risks from the perspective of drug development and disease. Liraglutide, a GLP 1 agonist for the treatment of diabetes, is a conjugated peptide that forms oligomers that can be stabilized by pH and organic solvents. We have developed an analytical toolkit to overcome challenges inherent to Liraglutide's conjugated acyl chain and probed the impact its oligomers have on its physical stability. Our studies show that Liraglutide's oligomer states have significant and potentially detrimental impacts on its propensity to aggregate and form fibrils as well as its potency. Liraglutide delivered as a synthetic peptide is able to maintain its oligomerization state in dried lyophilized powders, acting as a memory effect from its synthetic process and purification. Through Liraglutide's oligomer memory effect, we demonstrate the importance and impact the process for synthetic peptides can have on drug development spanning from discovery to formulation development.

**KEYWORDS:** fibrillation, aggregation, secondary structure, size exclusion chromatography, CD spectroscopy, bioassay



Peptides are important and complex modalities for pharmaceutical development, and approvals of new molecular entities for therapeutic treatments have rapidly risen over the past decade.<sup>1–3</sup> Continued breakthroughs in chemistry for peptides and proteins will enable greater exploration of an expanded chemical space for developing new therapeutics.<sup>4</sup> A key structural element common to peptide based therapeutics is the addition of a conjugate to the peptide core to enhance its pharmaceutical properties. Some benefits of conjugation can include tuning the peptide's in vivo half life or improving solubility.<sup>5</sup> In addition to enhancing pharmaceutical properties, incorporation of conjugates can significantly impact the physical state and stability of the peptide in the final formulated drug product ultimately dosed in patients. Over the course of a formulated peptide's shelf life, there is potential risk that the peptide may have a propensity to aggregate or form fibrils.<sup>6</sup> These pathways of physical instability are undesirable due to their potential risk of immunogenic responses and impacting bioavailability and efficacy.<sup>6,7</sup> The complex structural landscapes available to peptides and their associated risks necessitate that robust analytical methods are developed to characterize and understand their stability to ensure stable formulated drug products are delivered to patients.

A major and currently expanding class of therapeutic peptides are those that target the GLP 1 receptor for the

treatment of diabetes.<sup>8–11</sup> Several peptides that are marketed or in development are conjugated to allow dosing for different durations ranging from once daily to once weekly.<sup>11</sup> For example, the GLP 1 agonist Liraglutide's primary structure mimics the natural GLP 1 hormone with the exception of a single amino acid mutation at its N terminus and the inclusion of a C16 acyl conjugation (Figure S1). The natural GLP 1 peptide hormone, that which several therapeutic peptides resemble, is known to have a complex structural landscape including a high propensity to aggregate and form fibrils.<sup>12–14</sup> Recently, it was shown that the GLP 1 peptide is one of a few known peptides reported in the literature to have unique pH dependent fibrillation properties.<sup>14</sup> Generally, peptides that undergo fibrillation do so in a concentration dependent manner where increasing peptide concentration results in enhanced fibrillation kinetics.<sup>15,16</sup> In stark contrast, the GLP 1 peptide shows an inverse concentration dependence at pH < 7, where it has a tendency to form fibrils more rapidly at low concentrations. Beyond the unique aspects of the GLP 1 peptide's pH dependent fibrillation properties, Liraglutide has been shown to form soluble oligomers that vary in size as a

Received: January 23, 2019

Revised: April 13, 2019

Accepted: April 16, 2019

Published: April 16, 2019

function of pH.<sup>17</sup> Similar to the GLP 1 fibrillation concentration dependence, the oligomerization state of Liraglutide differs depending on if the solution pH is acidic or basic.

Here, we sought to probe whether Liraglutide, with the addition of its conjugation and pH dependent oligomerization, maintains the unique fibrillation properties that have recently been identified for GLP 1. To characterize Liraglutide, we have deployed an analytical toolkit including size exclusion chromatography (SEC) coupled with light scattering detection, kinetic fibrillation/aggregation experiments, transmission electron microscopy, circular dichroism spectroscopy, and bio assay. Through our characterization studies, we show that similar to GLP 1, Liraglutide exhibits unique concentration dependent fibrillation and aggregation kinetics as a function of pH.<sup>14</sup> During development of our characterization techniques, it became apparent that control of Liraglutide's pH dependent oligomerization state was crucial for its physical stability. Our studies show that Liraglutide is able to maintain its oligomer state in lyophilized powders, the form in which most synthetic peptides are delivered. Liraglutide's oligomer states can significantly impact its propensity to form fibrils, aggregate, and its biological potency. Previous work on recombinant GLP 1 peptides has shown the synthetic process can have impacts on solubility and generation of undesirable aggregates.<sup>18,19</sup> Given Liraglutide's oligomer memory, our studies highlight the importance of controlling and understanding the process used in synthetic peptide synthesis and purification and its potential downstream impacts that span from discovery to preclinical development and formulation activities.

## ■ EXPERIMENTAL SECTION

**Materials.** Liraglutide was purchased from Bachem (Torrance, CA) with a potency of 97.5% and used without further purification. The Bachem sourced Liraglutide was used for all studies with the exception of those specifically noted. Liraglutide was purchased from Achemblock (Burlingame, CA) with a purity of 99.4% and used without further purification. Liraglutide peptide powder was reconstituted with 50 mM sodium phosphate adjusted to the desired pH with sodium hydroxide. All other chemicals used in this study were reagent grade or better.

**Size-Exclusion Chromatography.** Experiments were carried out on a variety of HPLC/UHPLC systems including Waters Acquity UPLCs, Agilent 1290s, and Agilent 1200s controlled using Empower 3. The columns used for SEC experiments included the Sepax Unix C 300 Å pore size 4.6 × 150 mm (UHPLC) and Sepax SRT C 300 Å pore size 7.8 × 300 mm (HPLC). The mobile phase was 10 mM sodium phosphate at a pH of 6.4 or 8.1. Note, because of the slow kinetics of the oligomer transition, the populations of States A and B were not significantly impacted by the mobile phase pH. Flow rates were 0.3 and 1.0 mL/min for UHPLC and HPLC, respectively. The LC sample tray was set to 5 °C for all sample analysis with the exception of 25 °C for incubation studies. UV detection for UHPLC/HPLC was carried out at 280 nm, and corresponding peak areas were used for oligomer population determination. HPLC SEC experiments included online detection of multiangle light scattering (MALS), quasielastic light scattering (QELS/DLS), and refractive index using Wyatt Dawn Heleos II, Wyatt Nanostar, and Wyatt Optilab Trex detectors. We measured and used the refractive index increment of  $dn/dc = 0.186 \text{ mL/g}$  for Liraglutide (matches within 2% of a recent study) with a Wyatt Optilab Trex.<sup>17</sup>

Analysis of light scattering data was carried out using Wyatt ASTRA 6.1.7.15.

**Lyophilization.** Liraglutide samples were prepared by reconstituting the Liraglutide lyophilized powder with 50 mM sodium phosphate at the desired pH (6.4, 6.7, 8.1). Samples were allowed to incubate at 25 °C for 43 h to achieve their equilibrium oligomer distribution. The equilibrated samples were then lyophilized using an SP Scientific VP 60X lyophilizer. The lyophilized samples were reconstituted with water and immediately assayed by SEC.

**Fluorescence and Kinetic ThioT Experiments.** Liraglutide samples were prepared by reconstituting the lyophilized peptide with 50 mM sodium phosphate at the desired pH (6.4–8.1) at a concentration of 8 mg/mL with gentle stirring until the peptide went into solution. The additional concentrations of 1–4 mg/mL were prepared by diluting the 8 mg/mL Liraglutide stock with 50 mM sodium phosphate at the desired pH. Samples were then transferred to a 96 well plate with a total sample volume of 200 μL with 5 μM thioflavin T (ThioT). Physical stress and fluorescence detection (excitation = 440 nm and detection = 480 nm) were carried out using a Spectramax M2. Samples were constantly stressed by shaking at 25 °C, and ThioT fluorescence was recorded every 5 min.

**Transmission Electron Microscopy.** Images of peptide fibrils were obtained on an FEI Tecnai Spirit Biotwin transmission electron microscope at a voltage of 120 kV. All peptide solutions were diluted to 1 mg/mL as necessary with water. A 5 μL aliquot of the 1 mg/mL peptide solution was deposited on the surface of a 200 mesh carbon coated copper grid. After 1 min, excess liquid was blotted away with filter paper, and the grid was rinsed briefly with 5 μL of water. The rinsewater was wicked away with filter paper, and 5 μL of 1% uranyl acetate was then added to the grid as a negative stain to enhance contrast. After 1 min, excess stain was blotted away, and the grids were imaged immediately.

**Circular Dichroism Spectroscopy.** Circular dichroism spectra were acquired on a Chirascan qCD Spectrophotometer (Applied Photophysics, Surrey, UK). The temperature was maintained at 25 °C during the course of the measurement, consisting of two repetitions scanning from 200 to 280 at 1 nm bandwidth. Solid Liraglutide was dissolved to a concentration of 1 mg/mL in 50 mM sodium phosphate at the desired pH value (6.4, 6.7, and 7.2). These solutions were allowed to stand at room temperature over the course of the experiments. Aliquots (75 μL) were removed from the solution and further diluted 4× with buffer to a final concentration of 0.25 mg/mL before acquisition of CD spectra. This dilution was necessary to bring the total absorbance below 1 AU for the entire spectral range. The final time course spectra were normalized to the initial time point before comparison. For the experiments pertaining to addition of organic solvent, the same procedure was followed with the exception of the initial Liraglutide solutions, which were made with 10% of either EtOH or TFE. For analysis of kinetic data, we assumed Liraglutide CD spectra to be a linear combination of States A and B

$$\theta_{\text{exp}} = \alpha \cdot \theta_A + \beta \cdot \theta_B \quad (1)$$

where  $\theta_{\text{exp}}$  is the experimental CD spectrum,  $\alpha$  is the percentage of State A,  $\theta_A$  is the State A reference CD spectrum,  $\beta$  is the percentage of State B, and  $\theta_B$  is the State B

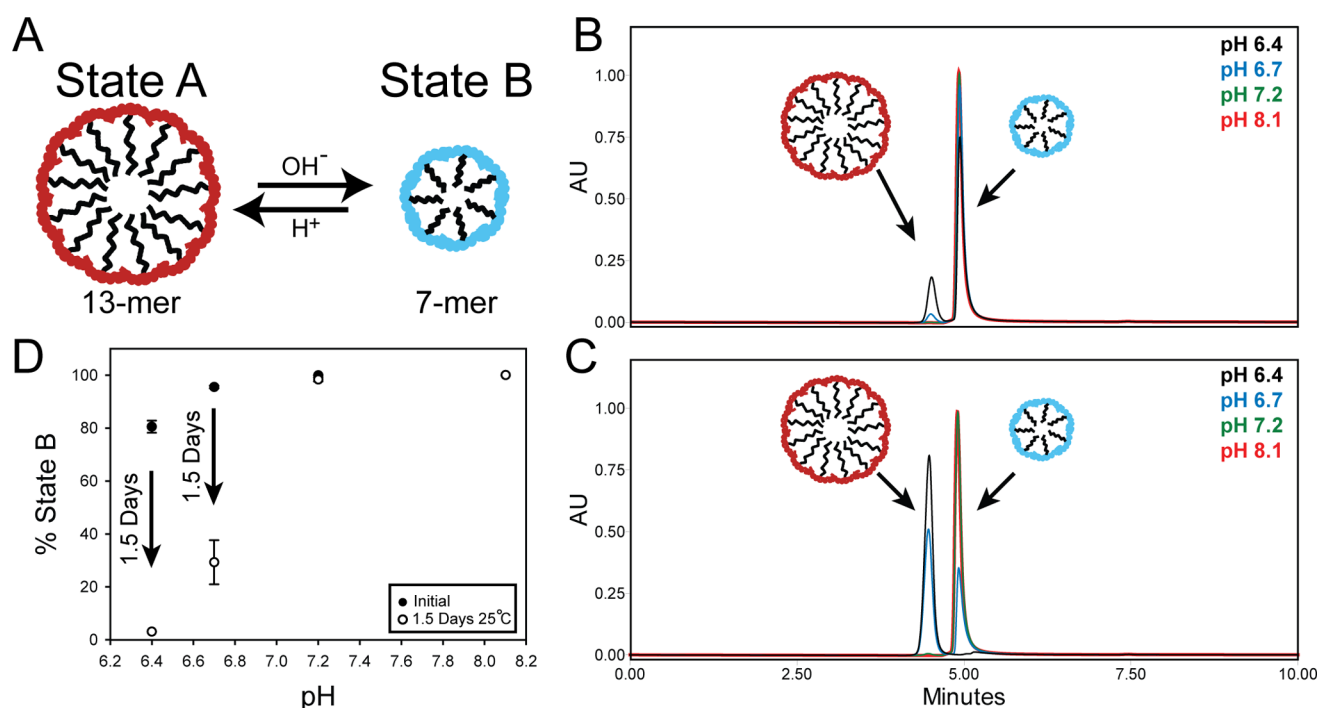


**Figure 1.** Characterization of Liraglutide oligomerization by SEC. (A) Liraglutide exists as two different oligomerization states that are stabilized by acidic or basic conditions. (B) SEC chromatograms of 4 mg/mL Liraglutide solutions at pH 6.4–8.1 recorded immediately after preparation. (C) SEC chromatograms of 4 mg/mL Liraglutide solutions at pH 6.4–8.1 recorded after incubation at 25 °C for 1.5 days. (D) Population of State B determined by SEC peak areas immediately after preparation (filled circles) and after incubation at 25 °C for 1.5 days (open circles).

reference CD spectrum. Eq 1 was fit using the “Non LinearModelFit” function built into Wolfram Mathematica 8.

**Cell Based Potency Assay.** The bioassay method used was based on Cisbio’s HTRF technology (Homogeneous Time Resolved Fluorescence) for quantitative measurement of cyclic AMP using Cisbio’s cAMP Dynamic 2 reagents with Chinese hamster ovary (CHO) cells stably expressing the glucagon like peptide 1 receptor (CHO GLP1R) cells. As a G protein coupled receptor, GLP 1 receptor mediated signaling involves activation of the adenylate cyclase component of GLP 1 receptor, which increases the level of cAMP (adenosine 3’,5’ cyclic mono phosphate).<sup>20</sup>

The bioactivity of samples was tested in a bioassay immediately after preparation of Liraglutide samples at pH 6.4 and 8.1 that primarily populate State B. The pH 6.4 sample was in a kinetic oligomer distribution at pH 6.4, primarily populating State B (Figure 1D). Bioactivity was also tested for samples that had been allowed to incubate at 25 °C for 3 days. Here, the pH 6.4 sample had achieved equilibrium primarily populating State A. A freshly prepared sample at pH 8.1 was used as a reference to compare the potency values of the samples at pH 6.4 (immediate and 3 day, 25 °C) and 8.1 (3 days, 25 °C). Percent relative potency values (reference  $IC_{50}$ /sample  $IC_{50} \times 100$ ) were determined from the comparison of the reference and test sample using a 4 PL curve fit. The  $IC_{50}$  value obtained from the curve represents the concentration of Liraglutide that inhibits 50% of the maximum response.

## RESULTS AND DISCUSSION

**Characterization of Liraglutide Oligomerization.** It was recently reported that Liraglutide can populate two oligomerization states that are stabilized by varying pH (Figure 1A).<sup>17</sup> At pH < 7, Liraglutide was shown to exist as a 12 mer

by dynamic light scattering (DLS) and static light scattering (SLS). While under basic conditions, Liraglutide has been shown to exist as either an 8 mer<sup>17</sup> or 7 mer<sup>21</sup> depending on the technique used (light or small angle X ray scattering (SAXS)). While DLS, SLS, and SAXS were able to provide deep insights into the oligomerization of Liraglutide, the interpretation and deconvolution of light/X ray scattering data has significant limitations for cases such as Liraglutide, where it is possible that multiple states with differing size can simultaneously exist in solution at near neutral pH.<sup>22–25</sup>

To overcome challenges inherent to light scattering measurements of bulk solutions, we sought to develop a size exclusion chromatography method able to separate the oligomerization states of Liraglutide. Achieving separation of the oligomerization states would allow for accurate determination of their populations and enable additional on or offline analysis by techniques such as light scattering or mass spectrometry. Separation of conjugated peptides is notoriously challenging due to their conjugation chemistries having a tendency to cause undesirable secondary interactions with column stationary phases. This is particularly the case for acylated peptides where a greasy carbon chain (C16 for Liraglutide) is covalently attached. Addition of organic solvents in some cases can help to minimize secondary interactions but are not ideal, because they could disrupt or generate aggregates/oligomers on column. Initial SEC method screening with a pure aqueous mobile phase showed a challenge in achieving conditions that minimized secondary interactions between Liraglutide and the stationary phase (Figure S2). Through our screen, we identified that by utilizing Sepax “C series” columns (UHPLC/HPLC) we could achieve conditions with minimal secondary interactions, good peak shape, and most importantly separation of the oligomerization states of Liraglutide. The stationary phase of these columns has a

proprietary lay down nanometer film chemically bonded to the silica particles likely minimizing Liraglutide's undesirable secondary interactions.

With the Sepax SEC method in hand, we were able to demonstrate the separation of two distinct oligomerization states (Figure 1B) that are stabilized as a function of pH consistent with a recent report by Wang et al.<sup>17</sup> State A is stable at pH < 7, and State B is stable at pH > 7 (Figure 1A). Separation of the individual states allowed us to probe their structure with online DLS and MALS detection (Figure 1B). The hydrodynamic radius for each state ( $R_{h,A} = 3.4 \pm 0.3$  nm and  $R_{h,B} = 2.6 \pm 0.2$  nm) was in agreement with the radii recently reported for each species by bulk DLS,<sup>17</sup> confirming that the oligomerization states of States A and B observed on column are the same as in bulk solution. Molecular weight analysis of the individual species using MALS showed that State A exists as a 13 mer ( $13.0 \pm 0.5$ ), and State B exists as a 7 mer ( $6.7 \pm 0.6$ ), consistent with the sizes recently reported as 12 mer (State A) and 8 mer or 7 mer (State B).<sup>17,21</sup> The differences observed in reported molecular weights are likely attributable to error and analysis differences between SEC MALS, bulk SLS, and SAXS. The combined light scattering data supports that the species observed by SEC are representative of the oligomers in bulk solution. Further, it was previously reported that the kinetics of the transformation between States A and B is slow, occurring on the time scale of days.<sup>17</sup> Our SEC results were consistent with pH driven transitions being slow on the SEC time scale, where the mobile phase pH did not significantly impact the populations of States A and B calculated from the oligomer peak areas.

Surprisingly, upon preparation of Liraglutide samples expected to favor State A at pH 6.4 by reconstitution with sodium phosphate buffer, we observed State B to be the initial primarily populated state (Figure 1B). After the samples were allowed to equilibrate at room temperature for several days, the system achieved equilibrium with Liraglutide transitioning to fully populate the thermodynamically favored State A (Figure 1C). We tested synthetic Liraglutide sourced from another vendor and saw a similar effect (Figure S3). The observation of an initial kinetic distribution of Liraglutide upon reconstitution of the lyophilized peptide powder led to the hypothesis that either the thermodynamically unfavored State B could be kinetically favored upon hydration of the dry powder or that the Liraglutide oligomer immediately populated in solution is a memory effect from its prelyophilized state. In order to distinguish between the two scenarios, we prepared Liraglutide solutions that populated different distributions of States A and B (pH 6.4, 6.7, 8.1) and lyophilized the solutions after they had achieved their oligomer thermodynamic equilibrium. Similar to our initial experiment, we assayed the oligomer distribution immediately after reconstitution of the lyophilized samples with water. Interestingly, samples that had favored State B upon reconstitution of the "as is" purchased lyophilized powder now populated their thermodynamically favored oligomer distributions observed prior to our lyophilization (Figure 2). Through the lyophilization process, the oligomer distribution was not impacted by any sodium phosphate acidic pH swing that occurred during freezing<sup>26</sup> because of the slow oligomer transformation kinetics that are likely even slower at subzero temperatures. This demonstrates that Liraglutide has an oligomer "memory effect", where the oligomerization states in solution prior to lyophilization are maintained in the

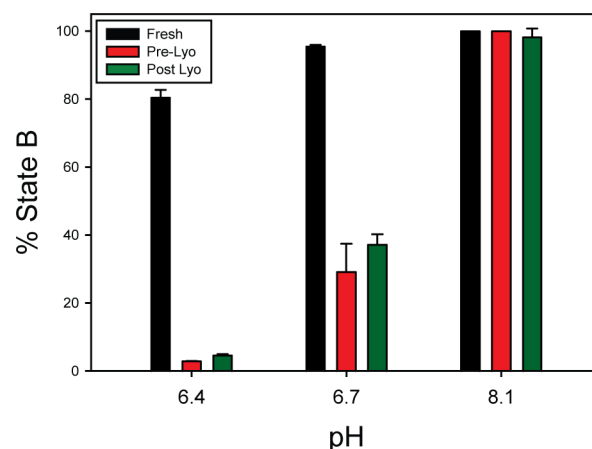


**Figure 2.** Populations of Liraglutide State B before and after lyophilization at varying pH. Fresh (black): Liraglutide population after reconstitution of the peptide powder with 50 mM sodium phosphate; Pre Lyo (red): Liraglutide State B population after incubation at 25 °C for 43 h prior to lyophilization; Post Lyo (green): Liraglutide State B population immediately after reconstitution of the Lyo cake with water.

lyophilized powder and populated upon hydration into solution.

**Oligomerization Impact on Physical Stability.** Given our observation of the oligomer "memory effect", we sought to probe the impact oligomer states could have on the physical stability of Liraglutide. To examine the physical stability and tendency to form fibrils and aggregate, we carried out studies catalyzing fibrillation and aggregation with physical stress using ThioT fluorescence as a reporter of fibril formation. Liraglutide stress studies were done using concentrations of 1–8 mg/mL at pH 6.4–8.1 employing physical stress by shaking at 25 °C. Shown in Figure 3 are the resulting fluorescence profiles for stressed Liraglutide at 25 °C for pH 6.4 and 8.1 where fluorescence increases upon ThioT binding fibrils or aggregates. Liraglutide exhibits an interesting concentration dependence at pH 6.4 (Figure 3A) where fibrillation occurs more rapidly as concentration decreases. This is similar to a recent report on the natural GLP 1 hormone, for which a similar concentration dependence is observed at pH < 7.<sup>14</sup> It is interesting that Liraglutide is able to maintain this unique property despite the addition of a bulky conjugate, mutation at the N terminus, and formation of oligomers in solution. This rare inverse concentration dependence has only been reported for a few peptides.<sup>14,27,28</sup> At a basic pH of 8.1 (Figure 3B), Liraglutide exhibits more rapid fibrillation with increasing concentration, which is the classical concentration dependence typically observed for fibrillation.<sup>15,16,29</sup>

In addition to the unique concentration dependence observed at pH 6.4, the oligomerization state of Liraglutide plays a significant role in its tendency to form fibrils and aggregate. Utilizing our knowledge of Liraglutide oligomerization from SEC and our ability to control the populations of each oligomer, we carried out studies to probe the impact of the initial oligomer state of the system (kinetic or equilibrium) on aggregation and fibrillation. First, we compared the ThioT profile for Liraglutide samples immediately prepared at pH 6.4 that exist in a kinetic oligomer distribution where State B is primarily populated (populated at ~80%) and samples that had been allowed to achieve equilibrium fully populating State A prior to stress. As shown in Figure 3A, the ThioT profiles are

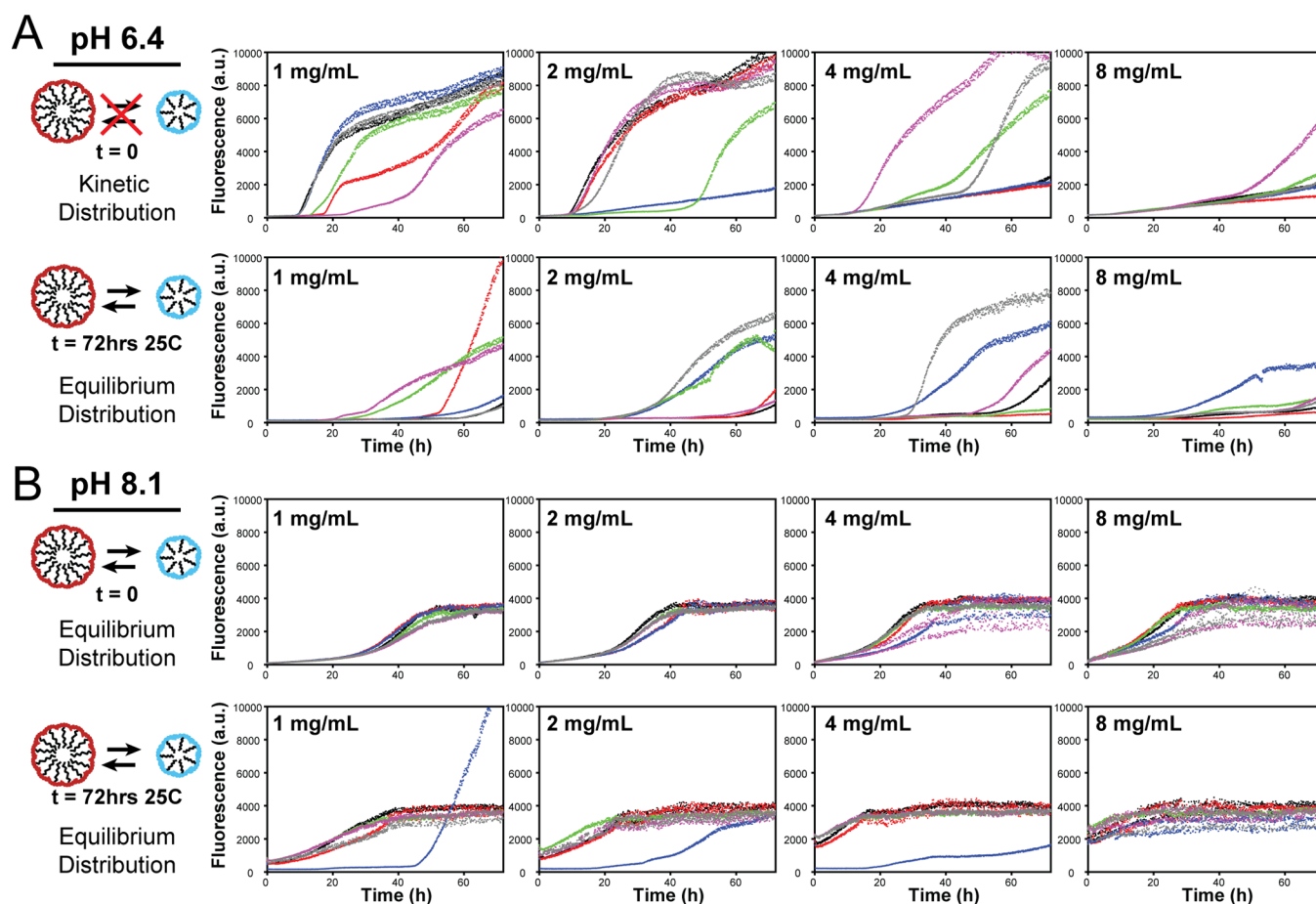


**Figure 3.** Fibrillation/aggregation of 1–8 mg/mL Liraglutide solutions upon immediate sample preparation and after incubation at 25 °C for 3 days. Six replicates were recorded, and each replicate is a different color. (A) ThioT fluorescence profile recorded during physical stress of Liraglutide solutions at pH 6.4 immediately after preparation (top) and after incubation at 25 °C for 3 days (bottom). (B) ThioT fluorescence profile recorded during physical stress of Liraglutide solutions at pH 8.1 immediately after preparation (top) and after incubation at 25 °C for 3 days (bottom).

drastically different between the samples in kinetic or equilibrium distributions particularly at low concentrations. Samples that were stressed while in a kinetic oligomer distribution at 1 mg/mL underwent more rapid changes in fluorescence than those that were allowed to achieve their equilibrium state prior to stress (Figure 1). We also observed a similar effect at pH 6.7 where samples stressed beginning with a kinetic distribution had much more rapid increases in fluorescence compared to those with an equilibrium oligomer distribution (Figure S4). In contrast to the samples that contain State A (pH 6.4 and 6.7), samples at a pH > 7 that exclusively populate State B upon reconstitution and at equilibrium became less stable as the samples aged. At pH 8.1, samples stressed immediately after preparation underwent ThioT fluorescence changes slower than samples allowed to incubate at 25 °C for 3 days (Figure 3B). SEC MALS analysis of pH 8.1 samples aged at 25 °C for 3 days showed that high molecular weight aggregates were present at the initiation of the fibrillation experiments, having formed during the incubation period. It is possible that these aggregates could give rise to the higher initial fluorescence and more rapid fibrillation. Liraglutide samples at pH 7.2, only populating State B, also showed decreasing stability after the samples had aged for 3 days (Figure S4).

These combined data from pH 6.4–8.1 show that Liraglutide's fibrillation and aggregation characteristics are modulated both by the populations of each oligomer state and whether the system is in thermodynamic equilibrium prior to initiating physical stress. Systems (pH 6.4 and 6.7) with a kinetic oligomer distribution were significantly less stable where they were undergoing oligomer conformational transformations during physical stress. The ThioT profiles are complex particularly at low pH having variable lag times, multiple phases in fluorescence increase, and a lack of signal plateauing. These complexities preclude global fitting of the data to a specific fibrillation or aggregation mechanism.<sup>30</sup> However, it is clear at low pH that when the oligomer distribution is not at equilibrium, Liraglutide has enhanced physical instability with an inverse concentration dependence. When under kinetic oligomer conditions, transformation from State B to State A may enable faster fibrillation and aggregation because of the presence of a catalyzing intermediate state. The inverse concentration presence for fibril formation could be from high concentrations of State B that play an inhibitory role in the fibrillation/aggregation process favored at acidic pH's.

The unique ThioT profiles observed for Liraglutide necessitated a deeper look with orthogonal methods to better understand the species that had formed upon stress. Increases in ThioT fluorescence are indicative of conformational

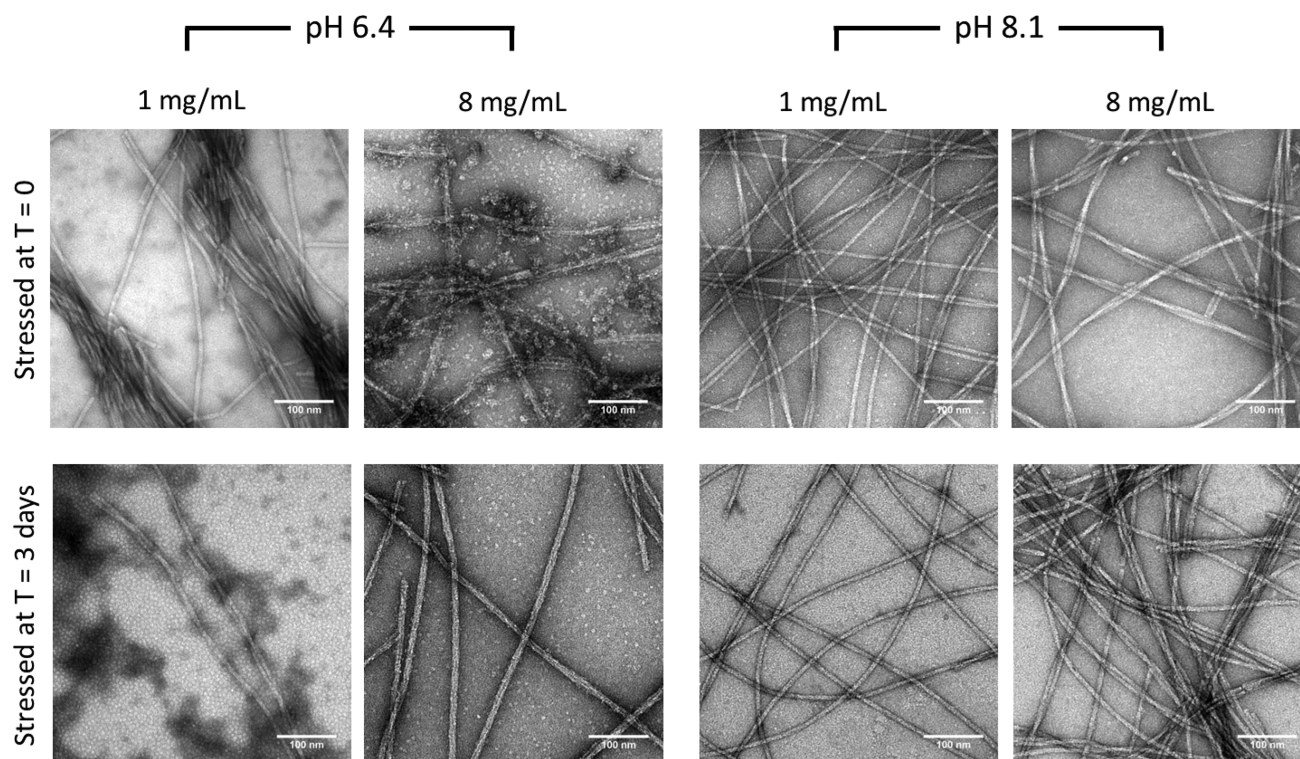


**Figure 4.** TEM micrographs of Liraglutide fibrils after stress.

changes; however, the fluorescence increase could be due to fibrillation, formation of aggregates that bind ThioT, or both.<sup>31</sup> To probe aggregate formation, we captured and assayed samples by SEC at pH 6.4 and 8.1 over the course of the ThioT fluorescence profiles (Figure S5). Interestingly, pH 6.4, samples stressed in a kinetic oligomer distribution had a higher tendency for aggregate formation at lower Liraglutide concentrations. The aggregates detected were  $\sim 20$ – $30$  MDa in size with  $R_h$ 's and  $R_g$ 's of  $\sim 50$  and  $\sim 100$ – $150$  nm, respectively. The ratio of  $R_g$  and  $R_h$  of  $\sim 2$ – $3$  suggests that these aggregates are rod like. Further, formation of significant high molecular weight aggregates at 1 mg/mL correlated with the timing ( $\sim 20$  h) of significant increases in ThioT fluorescence (Figure 3A). Samples at pH 6.4 incubated at 25 °C prior to stress had different aggregation properties where significant aggregation was delayed and increased with increasing concentration (Figure S5). In contrast, pH 8.1 aggregates had a significantly broader SEC peak shape than those formed at pH 6.4 (Figure S5). pH 8.1 aggregates formed more readily with increasing concentration with differing size of  $\sim 15$  MDa and  $R_h$ 's and  $R_g$ 's of  $\sim 60$  and  $\sim 150$  nm, respectively. Overall, SEC characterization of soluble species demonstrated stress induced formation of high molecular weight aggregates that have pH/oligomerization dependent properties and become significantly populated as ThioT fluorescence increases.

Next, we characterized the samples poststress by TEM imaging to probe if fibril morphology was dependent on pH and the equilibrium state of Liraglutide oligomers when stressed. Single Liraglutide fibrils are approximately 7 nm in width with distinct pH and concentration dependent morphological differences (Figure 4). At pH 6.4, 1 mg/mL Liraglutide solutions developed fibrils that exist in higher order bundles among unstructured peptide aggregates. Increasing the peptide concentration to 8 mg/mL led to a more defined

network where bundled fibers are composed of two to three individual fibrils. At pH 8.1, 1 mg/mL Liraglutide solutions formed well defined single fibrils that occasionally intertwine together. This intertwined morphology becomes more prevalent in samples at elevated concentrations. The fibril morphologies observed at a given pH and peptide concentration do not differ substantially when comparing samples stressed in a kinetic or equilibrium oligomer distribution, despite the significant differences observed in the ThioT assay. This suggests that the final fibular state is less governed by the kinetic assembly but rather the molecular interactions between peptides that are linked to pH and peptide concentration. These unique peptide interactions at the molecular level extend to the macroscale morphology of the peptide fibril as observed in both synthetic<sup>32</sup> and natural<sup>33</sup> fibril forming peptides.

By characterizing and controlling Liraglutide's oligomers in either a kinetic or equilibrium distribution, we were able to probe their impact on Liraglutide's physical stability. Overall, the aggregation/fibrillation data shows that both the oligomer identity and status of thermal equilibrium from the oligomer "memory effect" can play major roles in fibrillation/aggregation kinetics under physical stress.

**Oligomer Structure and Driving Forces for Stabilization.** Because Liraglutide's oligomers play such an important role in its tendency to aggregate and form fibrils, we probed their secondary structure using CD spectroscopy. A recent study showed that the CD spectrum of State A is a mixture of secondary structural elements, and State B is primarily  $\alpha$  helical.<sup>17</sup> As shown in Figure 5A, CD spectra of Liraglutide samples fully populated in State A (pH 6.4) or State B (pH 7.2) were consistent with the previous work by Wang et al.<sup>17</sup> We have shown by SEC that Liraglutide's oligomer distribution is maintained in its dried lyophilized powder form. This led us to inquire if Liraglutide's secondary structure was also

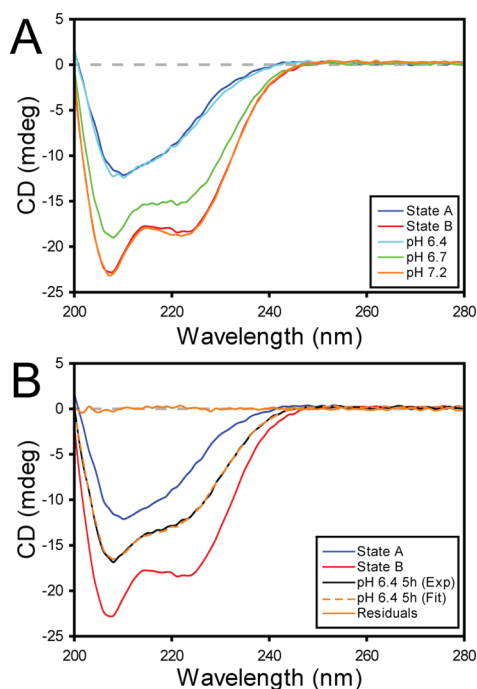


**Figure 5.** CD analysis of Liraglutide solutions. (A) CD spectra of Liraglutide solutions at varying pH as indicated in the legend. Reference spectra for pure States A and B are shown. (B) Analysis of Liraglutide at pH 6.4, 5 h post reconstitution during conversion to State A. The resulting linear combinations of pure States A and B are shown in orange along with residuals.

maintained with its oligomer distribution upon reconstitution. Could Liraglutide immediately form the thermodynamically favored secondary structure in solution while simultaneously existing a nonfavored oligomer state? To address this question, we carried out CD experiments of freshly prepared Liraglutide samples at pH 6.4 and 6.7 that exist in a kinetic distribution initially populating oligomer State B. CD spectra recorded immediately after reconstitution at pH 6.4 and 6.7 are primarily  $\alpha$  helical, consistent with the CD spectrum of State B. This CD data of samples in a kinetic oligomer distribution confirms that the secondary structure is linked to the oligomer forms State A and B.

Kinetic CD data monitoring the structural transition from State B to A upon reconstitution was also consistent with the time scales observed by SEC and reported by Wang et al.<sup>17</sup> In order to gain understanding of the change from State B to State A and determine if this transition was proceeding directly from State B to State A or via a structural intermediate, we examined time course data for all pH values more closely. To probe for the presence of a structural intermediate, we fit kinetic CD data with linear combinations of State A and State B (Figure 5B). For example, data recorded 5 h postpreparation at pH 6.4 resulted in an excellent fit of the kinetic CD spectrum with 44.4% State B (Figure 5B). Given that kinetic CD spectrum could be simply described by reference spectra of States A and B, we were unable to detect an intermediate state. This analysis was repeated for kinetic data points at pH 6.4 and 6.7 with similarly good agreement between predicted and experimental values. A previous report proposed the mechanism of oligomer transformation to be driven by monomer dissociation and reassembly of oligomers.<sup>17</sup> While we were unable to observe an intermediate within the

detection limits of our CD and SEC experiments, we cannot exclude any proposed mechanism.

Our observations confirmed that secondary structure was distinctly linked to each oligomer state and that there are likely key structure driven contacts that stabilize each oligomer state. Next, we tested if it was possible to modulate the oligomer distribution of Liraglutide by factors other than pH. Previous structural studies of the natural GLP 1 hormone have used trifluoroethanol<sup>34</sup> (TFE) to stabilize an  $\alpha$  helical conformation allowing for structural determination and analysis by NMR.<sup>35,36</sup> Similarly, a recent report showed that TFE could enhance Liraglutide's  $\alpha$  helical structural content by CD.<sup>37</sup> Addition of 10% TFE to Liraglutide at pH 6.4 and 6.7 drove its CD spectrum to be primarily composed of  $\alpha$  helical structure, and SEC confirmed that State B had been fully populated at each pH (Figure S6). To further probe the impact of organic solvents on Liraglutide's conformation, we carried out a similar study adding ethanol from 10 to 35% at pH 6.4 and 6.7. Although the change in oligomer populations was not as drastic as TFE, ethanol had a similar effect in stabilizing State B. Increasing the ethanol concentration to 35% pushed Liraglutide to fully favor State B at pH 6.4 and 6.7 (Figure S6). Addition of either TFE or ethanol at varying levels further showed that Liraglutide readily populates two distinct states with specific secondary structure. Overall, the ability of organic solvents to change Liraglutide's oligomer distribution demonstrates that Liraglutide's favored oligomerization state can be modulated by factors other than pH.

#### Formulation Excipient Impact on Oligomerization.

Our experiments probing the driving forces for oligomer stabilization showed that alcohols could significantly influence the oligomerization state of Liraglutide. This led us to question if excipients in a formulated drug product could influence Liraglutide's oligomerization state. Multiuse injectable formulations include an antimicrobial agent and also commonly have a tonicity modifying agent. It has been shown for other peptides and proteins that antimicrobial agents are notorious for negatively impacting long term physical stability.<sup>38–40</sup> To study the impact of excipients on Liraglutide's oligomerization state, we selected pH 6.4 (favoring State A) and pH 6.7 (mixture of State A and B) as test scenarios. In Figure 6, we focus on pH 6.7, and the pH 6.4 results are in Supporting

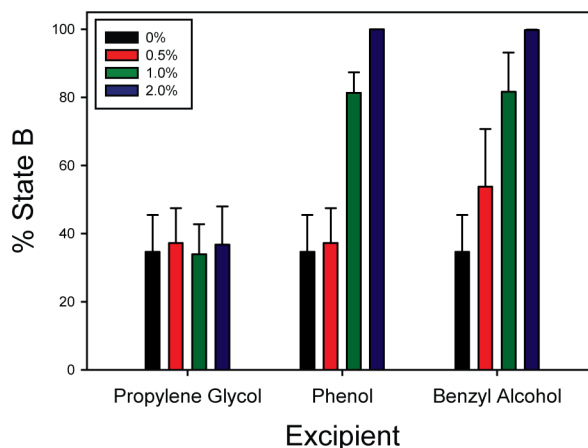


**Figure 6.** Influence of excipients on Liraglutide's oligomerization states. Shown are the populations of Liraglutide State B at pH 6.7 determined by SEC after storage of 2 mg/mL Liraglutide for 48 h at 25 °C with varying excipients (concentrations indicated in key).

**Table 1.** Bioassay Data of Liraglutide Samples ( $n = 8$ ) in Kinetic and Equilibrium Distributions Compared to a Reference Sample Immediately Tested after Preparation of 1 mg/mL at pH 8.1

sample	condition	major oligomer state	reference	geomean relative potency	%GSD	95% LCL	95% UCL
1 mg/mL, pH 6.4	3 days RT	A	pH 8.1 - fresh	70	13	63	78
1 mg/mL, pH 8.1	3 days RT	B	pH 8.1 - fresh	99	6	94	105
1 mg/mL, pH 6.4	fresh	B	pH 8.1 - fresh	103	4	100	107

**Information** (Figure S7). Propylene glycol is a commonly utilized tonicity modifier in sterile formulations. Addition of propylene glycol to solutions containing Liraglutide at pH 6.4 and 6.7 did not significantly change the populations of States A and B (Figures 6 and S7). In contrast, addition of the antimicrobial agents phenol and benzyl alcohol significantly altered Liraglutide's oligomerization, shifting the equilibrium to favor State B (Figure 6 and S7). Our results show that excipients commonly used in sterile formulations can significantly alter the equilibrium of Liraglutide's oligomerization states. Because antimicrobial agents drove the equilibrium toward State B, it could be difficult in development to find a formulation fully that fully populates State A. This study highlights the complex interplay and balancing act that can exist between peptides and excipients to stabilize a desired conformational state.

**Oligomerization Impact on Potency.** To probe the impact of Liraglutide's oligomerization state on potency, we carried out bioassay experiments on States A and B testing potency of samples that were under kinetic and equilibrium conditions. First, the bioactivity was tested immediately after preparation of Liraglutide samples at pH 6.4 and 8.1 that primarily populate State B and are in a kinetic distribution for pH 6.4 (Table 1). The bioactivity of each sample at pH 6.4 and 8.1 was statistically similar showing that State B has similar activity across differing pH. Next, we tested samples that had achieved their equilibrium distribution after storage for 3 days at room temperature (Table 1) where pH 6.4 populated State A and pH 8.1 populated State B. The potency value of the sample favoring State A was 70% relative to State B. Overall, the bioassay results not only reveal that State A is less potent than State B but also are consistent with our analytical measurements, sensitive to the populations and structures of Liraglutide's oligomer states. This data demonstrates the importance in characterization and control of these oligomerization states and their impact on biological potency.

## CONCLUSIONS

In conclusion, we have shown that Liraglutide exhibits unique pH and concentration dependent aggregation/fibrillation properties that are similar to GLP 1.<sup>14</sup> These unique fibrillation characteristics are maintained in Liraglutide despite the addition of a bulky acyl C16 conjugate and a single mutation at the N terminus. At pH < 7, Liraglutide forms aggregates/fibrils more rapidly with decreasing concentration, whereas at pH > 7, Liraglutide exhibits the commonly observed acceleration of fibrillation with increasing concentration. Further, our studies show the profound impact Liraglutide's two oligomerization states have on its physical stability and potency. The physical stability of Liraglutide can be linked to an oligomer memory effect from the process in which the peptide is manufactured/lyophilized. The influence of process on varying peptide attributes has been shown to be crucial for recombinant GLP 1's<sup>18,19</sup> and  $\beta$  amyloid<sup>41,42</sup> in the synthetic relm. When Liraglutide's oligomerization is in a

nonequilibrium state, it becomes more sensitive to physical stress. Liraglutide's oligomer States A and B can be stabilized by pH, organic solvents, and the addition of formulation excipients. Although the larger more structurally diverse State A has a lower tendency to form aggregates and form fibrils, it has a lower biological potency than the more structured State B. The contrast observed in stability and potency would need appropriate characterization for formulation selection requiring optimization of factors including concentration, choice of excipients, and manufacturing controls.<sup>43</sup>

Most importantly, our studies highlight the complex nature of developing synthetic peptides as pharmaceuticals and the multitude of challenges that could be faced from discovery through to clinical formulation development. With a functional analytical toolkit and resulting understanding of Liraglutide's complex oligomerization equilibrium in hand, we were able to dig into specific issues that could arise in varying stages in peptide development. Without an understanding of the synthetic process/purification impact and oligomerization state, good peptide candidates in development could be rejected because of observation of poor physical stability or a low biological potency. In the formulation and manufacturing space, a mismatch between the peptide synthetic process and drug product formulation manufacturing could lead to undesirable physical instability. This deep understanding from characterization is not always available in all stages of development; however, our studies demonstrate the utility in early investment and pursuit of robust analytical methods. In the case of Liraglutide, it has been possible to overcome physical stability challenges to develop stable formulated products including Victoza and Saxenda.

## ASSOCIATED CONTENT

### Supporting Information

The Supporting Information is available free of charge on the ACS Publications website at DOI: 10.1021/acs.molpharmaceut.9b00106.

Supporting Figures S1–S7 (PDF)

## AUTHOR INFORMATION

### Corresponding Author

\*E mail: jameson.bothe@merck.com.

### ORCID

Jameson R. Bothe: 0000 0002 1753 0994

Leo A. Joyce: 0000 0002 8649 4894

### Notes

The authors declare no competing financial interest.

## ACKNOWLEDGMENTS

The authors thank the peptide development teams within Pharmaceutical Sciences and Process Research and Development, W. Peter Wuelfing for helpful discussions, and Nicholas Marshall for help with the lyophilization experiments.



## ■ ABBREVIATIONS

SEC, size exclusion chromatography; MALS, multiangle light scattering; DLS, dynamic light scattering; SAXS, small angle X ray scattering; TEM, transmission electron microscopy; CD, circular dichroism; RT, room temperature; GSD, geometric standard deviation; LCL, lower confidence limit; UCL, upper confidence limit

## ■ REFERENCES

- (1) Lau, J. L.; Dunn, M. K. *Bioorg. Med. Chem.* **2018**, *26*, 2700.
- (2) Craik, D. J.; Fairlie, D. P.; Liras, S.; Price, D. *Chem. Biol. Drug Des.* **2013**, *81*, 136.
- (3) D'Addio, S. M.; Bothe, J. R.; Neri, C.; Walsh, P. L.; Zhang, J.; Pierson, E.; Mao, Y.; Gindy, M.; Leone, A.; Templeton, A. C. *J. Pharm. Sci.* **2016**, *105*, 2989.
- (4) deGruyter, J. N.; Malins, L. R.; Baran, P. S. *Biochemistry* **2017**, *56*, 3863.
- (5) Kontermann, R. E. *Curr. Opin. Biotechnol.* **2011**, *22*, 868.
- (6) Rosenberg, A. S. *AAPS J.* **2006**, *8*, E501.
- (7) Jiskoot, W.; Randolph, T. W.; Volkin, D. B.; Russell Middaugh, C.; Schoneich, C.; Winter, G.; Friess, W.; Crommelin, D. J.; Carpenter, J. F. *J. Pharm. Sci.* **2012**, *101*, 946.
- (8) Holst, J. J. *Physiol. Rev.* **2007**, *87*, 1409.
- (9) Madsbad, S.; Kielgast, U.; Asmar, M.; Deacon, C. F.; Torekov, S. S.; Holst, J. J. *Diabetes, Obes. Metab.* **2011**, *13*, 394.
- (10) Madsbad, S. *Diabetes, Obes. Metab.* **2016**, *18*, 317.
- (11) Yu, M.; Benjamin, M. M.; Srinivasan, S.; Morin, E. E.; Shishatskaya, E. I.; Schwendeman, S. P.; Schwendeman, A. *Adv. Drug Delivery Rev.* **2018**, *130*, 113.
- (12) Poon, S.; Birkett, N. R.; Fowler, S. B.; Luisi, B. F.; Dobson, C. M.; Zurdo, J. *Protein Pept. Lett.* **2009**, *16*, 1548.
- (13) Jha, N. N.; Anoop, A.; Ranganathan, S.; Mohite, G. M.; Padinhateeri, R.; Maji, S. K. *Biochemistry* **2013**, *52*, 8800.
- (14) Zapadka, K. L.; Becher, F. J.; Uddin, S.; Varley, P. G.; Bishop, S.; Gomes Dos Santos, A. L.; Jackson, S. E. *J. Am. Chem. Soc.* **2016**, *138*, 16259.
- (15) Nielsen, L.; Khurana, R.; Coats, A.; Frokjaer, S.; Brange, J.; Vyas, S.; Uversky, V. N.; Fink, A. L. *Biochemistry* **2001**, *40*, 6036.
- (16) Powers, E. T.; Powers, D. L. *Biophys. J.* **2006**, *91*, 122.
- (17) Wang, Y.; Lomakin, A.; Kanai, S.; Alex, R.; Benedek, G. B. *Mol. Pharmaceutics* **2015**, *12*, 411.
- (18) Senderoff, R. I.; Kontor, K. M.; Kreilgaard, L.; Chang, J. J.; Patel, S.; Krakover, J.; Heffernan, J. K.; Snell, L. B.; Rosenberg, G. B. *J. Pharm. Sci.* **1998**, *87*, 183.
- (19) Doyle, B. L.; Pollo, M. J.; Pekar, A. H.; Roy, M. L.; Thomas, B. A.; Brader, M. L. *J. Pharm. Sci.* **2005**, *94*, 2749.
- (20) Kuna, R. S.; Girada, S. B.; Asalla, S.; Vallentyne, J.; Maddika, S.; Patterson, J. T.; Smiley, D. L.; DiMarchi, R. D.; Mitra, P. *Am. J. Physiol. Endocrinol. Metab.* **2013**, *305*, E161.
- (21) Frederiksen, T. M.; Sonderby, P.; Ryberg, L. A.; Harris, P.; Bukrinski, J. T.; Scharff Poulsen, A. M.; Elf Lind, M. N.; Peters, G. H. *Biophys. J.* **2015**, *109*, 1202.
- (22) Philo, J. S. *AAPS J.* **2006**, *8*, E564.
- (23) Wen, J.; Arakawa, T.; Philo, J. S. *Anal. Biochem.* **1996**, *240*, 155.
- (24) Putnam, C. D.; Hammel, M.; Hura, G. L.; Tainer, J. A. *Q. Rev. Biophys.* **2007**, *40*, 191.
- (25) Konarev, P. V.; Svergun, D. I. *IUCrJ* **2018**, *5*, 402.
- (26) Gomez, G.; Pikal, M. J.; Rodriguez Hornedo, N. *Pharm. Res.* **2001**, *18*, 90.
- (27) Souillac, P. O.; Uversky, V. N.; Fink, A. L. *Biochemistry* **2003**, *42*, 8094.
- (28) Deva, T.; Lorenzen, N.; Vad, B. S.; Petersen, S. V.; Thorgersen, I.; Enghild, J. J.; Kristensen, T.; Otzen, D. E. *Biochim. Biophys. Acta, Proteins Proteomics* **2013**, *1834*, 677.
- (29) Ferrone, F. *Methods Enzymol.* **1999**, *309*, 256.
- (30) Meisl, G.; Kirkegaard, J. B.; Arosio, P.; Michaels, T. C.; Vendruscolo, M.; Dobson, C. M.; Linse, S.; Knowles, T. P. *Nat. Protoc.* **2016**, *11*, 252.
- (31) Biancalana, M.; Koide, S. *Biochim. Biophys. Acta, Proteins Proteomics* **2010**, *1804*, 1405.
- (32) Nagy Smith, K.; Moore, E.; Schneider, J.; Tycko, R. *Proc. Natl. Acad. Sci. U. S. A.* **2015**, *112*, 9816.
- (33) Paravastu, A. K.; Leapman, R. D.; Yau, W. M.; Tycko, R. *Proc. Natl. Acad. Sci. U. S. A.* **2008**, *105*, 18349.
- (34) Buck, M. *Q. Rev. Biophys.* **1998**, *31*, 297.
- (35) Chang, X.; Keller, D.; Bjorn, S.; Led, J. J. *Magn. Reson. Chem.* **2001**, *39*, 477.
- (36) Chang, X.; Keller, D.; O'Donoghue, S. I.; Led, J. J. *FEBS Lett.* **2002**, *515*, 165.
- (37) Guryanov, I.; Bondesan, A.; Visentini, D.; Orlandin, A.; Biondi, B.; Toniolo, C.; Formaggio, F.; Ricci, A.; Zanon, J.; Cabri, W. *J. Pept. Sci.* **2016**, *22*, 471.
- (38) Heljo, P.; Ross, A.; Zarraga, I. E.; Pappenberger, A.; Mahler, H. C. *Pharm. Res.* **2015**, *32*, 3201.
- (39) Meyer, B. K.; Ni, A.; Hu, B.; Shi, L. *J. Pharm. Sci.* **2007**, *96*, 3155.
- (40) Hutchings, R. L.; Singh, S. M.; Cabello Villegas, J.; Mallela, K. M. *J. Pharm. Sci.* **2013**, *102*, 365.
- (41) May, P. C.; Gitter, B. D.; Waters, D. C.; Simmons, L. K.; Becker, G. W.; Small, J. S.; Robison, P. M. *Neurobiol. Aging* **1992**, *13*, 605.
- (42) Dahlgren, K. N.; Manelli, A. M.; Stine, W. B., Jr.; Baker, L. K.; Krafft, G. A.; LaDu, M. J. *J. Biol. Chem.* **2002**, *277*, 32046.
- (43) Ludvigsen, S.; Schleim, M.; Bøving, T. E. G.; Bonde, C.; Lilleøre, A.; Engelund, D. K.; Nielsen, B. R. Stable Formulations of Insulinotropic Peptides. WO/2006/051110, EP1817048, 2014.